

A Chebychev propagator for inhomogeneous Schrödinger equations

Mamadou Ndong,¹ Hillel Tal-Ezer,² Ronnie Kosloff,³ and Christiane P. Koch^{1,*}

¹*Institut für Theoretische Physik, Freie Universität Berlin,*

Arnimallee 14, 14195 Berlin, Germany

²*Academic College of Tel-Aviv Yaffo, Israel*

³*Department of Physical Chemistry and The Fritz Haber Research Center,*

The Hebrew University, Jerusalem 91904, Israel

(Dated: July 30, 2019)

Abstract

We present a propagation scheme for time-dependent inhomogeneous Schrödinger equations which occur for example in optimal control theory or in reactive scattering calculations. A formal solution based on a polynomial expansion of the inhomogeneous term is derived. It is subjected to an approximation in terms of Chebychev polynomials. Different variants for the inhomogeneous propagator are demonstrated and applied to two examples from optimal control theory. Convergence behavior and numerical efficiency are analyzed.

*Electronic address: ckoch@physik.fu-berlin.de

I. INTRODUCTION

Inhomogeneous time-dependent Schrödinger equations,

$$i\hbar\frac{\partial}{\partial t}|\psi(t)\rangle = \hat{\mathbf{H}}|\psi(t)\rangle + \hat{\mathbf{G}}(t)|\varphi(t)\rangle, \quad (1)$$

arise in the time-dependent treatment of reactive scattering [1, 2] and in optimal control theory using time-dependent targets [3, 4, 5, 6] or state-dependent constraints [7]. In reactive scattering, the inhomogeneity results from the application of a projection operator [8]. This projector divides the Hilbert space of the reactive system into subspaces corresponding, respectively, to the reactants and to the products. A reduced description for only the products can be derived where the time-dependent Schrödinger equation contains an inhomogeneity, i.e. a source term that corresponds to the creation of the products [2]. In optimal control theory (OCT), the inhomogeneity is caused by the application of a projection operator as well, for example to suppress population in a subspace of the total Hilbert space [7]. This is formulated as a state-dependent constraint containing the projection operator. It gives rise to an inhomogeneity in the Schrödinger equation for backward propagation that corresponds to the suppression of probability amplitude in the forbidden subspace.

Generally, an inhomogeneous Schrödinger equation arises in OCT if a time-dependent target or a state-dependent constraint are utilized. In the common versions of OCT, see e.g. Refs. [9, 10], the target is not explicitly time-dependent, it depends only on some final time T . The constraints enforce the Schrödinger equation and a minimization of the field energy. But for explicitly time-dependent targets [3, 4, 5, 6] or for a state-dependent constraint [7, 11] the optimization functional contains a contribution of the form

$$\lambda \int_0^T g[\psi(t), \psi^*(t)] dt,$$

where the state $|\psi\rangle$ of the system enters at each time t .

For the solution of the standard homogeneous time-dependent Schrödinger equation, a number of numerical propagation schemes exist [12, 13]. The Chebychev propagator [14] offers the advantage of a numerically exact solution. The accuracy of the calculation is then determined by the machine precision of the computer and the error is uniformly distributed. The propagator is based on approximating the formal solution of the homogeneous time-dependent Schrödinger equation,

$$|\psi(t + dt)\rangle = e^{\frac{i}{\hbar}\hat{\mathbf{H}}dt}|\psi(t)\rangle, \quad (2)$$

by a series of Chebychev polynomials. Time-dependent inhomogeneous Schrödinger equations have been solved to date with split-propagator schemes [4] or via a full diagonalization of the Hamiltonian [7]. While the latter method is numerically expensive and quickly becomes unfeasible with increasing system size, the first is of only limited accuracy.

Here, we derive a formal solution of the time-dependent inhomogeneous Schrödinger equation and we adapt it to the Chebychev propagation scheme. We apply this new propagator to the optimal control with a state-dependent constraint and with a time-dependent target. The paper is organized as follows: Section II presents the formal solution of Eq. (1). Propagation schemes for the formal solution are derived in Section III. The Chebychev propagation scheme is applied to OCT with a state-dependent constraint where the system is forced to remain in a subspace of the total Hilbert space in Section IV. In this case the operator $\hat{\mathbf{G}}$ in Eq. (1) is independent of time, $\hat{\mathbf{G}}(t) = \hat{\mathbf{G}}$. In Section V, a second application, OCT with a time-dependent target, is studied keeping the full time-dependence, $\hat{\mathbf{G}}(t)$. In both applications, the convergence of the new Chebychev propagator is analyzed in detail. Section VI concludes.

II. FORMAL SOLUTION

The inhomogeneous Schrödinger equation, Eq. (1), is treated as an ordinary differential equation. It can be rewritten (setting $\hbar = 1$)

$$i \frac{\partial}{\partial t} |\psi(t)\rangle = \hat{\mathbf{H}} |\psi(t)\rangle + |\Phi(t)\rangle, \quad (3)$$

where $|\Phi(t)\rangle = \hat{\mathbf{G}}(t) |\varphi(t)\rangle$. Eq. (3) is solved with the boundary conditions

$$|\psi(0)\rangle = |\psi_0\rangle, \quad |\Phi(0)\rangle = |\Phi_0\rangle. \quad (4)$$

$|\Phi(t)\rangle$ is known globally in the propagation time interval, $[0, T]$, for example in a numerical representation on N_t sampling points. It is assumed to be analytic, so that it can be interpolated to any arbitrary point within $[0, T]$. The representation of $|\Phi(t)\rangle$ on N_t sampling points corresponds to an expansion in N_t basis functions. Choosing equidistant sampling points yields a Fourier representation. A high-order (usually $N_t \gg 1$) polynomial expansion is obtained when the sampling points are chosen as roots of polynomials, implying non-equidistant time steps. The optimal representation treating correctly the boundaries is obtained by choosing Chebychev polynomials.

The basic idea consists in devising a short-time integration scheme for the interval $[0, \Delta t]$ (or, more generally $[t_n, t_{n+1}]$ with $n, n+1 \leq N_t$) by taking the following polynomial expansion of the inhomogeneous term,

$$|\Phi(t)\rangle \approx \sum_{j=0}^{m-1} P_j(\bar{t}) |\bar{\Phi}_j\rangle \equiv \sum_{j=0}^{m-1} \frac{\bar{t}^j}{j!} |\Phi^{(j)}\rangle. \quad (5)$$

Here, P_j denotes the Chebychev polynomial of order j with expansion coefficient $|\bar{\Phi}_j\rangle$, and \bar{t} is a rescaled time, $\bar{t} = \frac{2t}{\Delta t} - 1$, for $t \in [0, \Delta t]$. The Chebychev expansion coefficients $|\bar{\Phi}_j\rangle$ could be evaluated for each time interval by interpolating the function $|\Phi(t)\rangle$ at the zeros of the m th Chebychev polynomial within the interval $[0, \Delta t]$ and performing a cosine transformation. Once the coefficients $|\bar{\Phi}_j\rangle$ are known they are used to generate the coefficients $|\Phi^{(j)}\rangle$ in the second sum of Eq. (5). This procedure has the advantage of employing a uniform approximation of $|\Phi^{(j)}\rangle$ in the interval $[0, \Delta t]$.

However, the uniform procedure was found hard to implement in applications where the function $|\Phi^{(j)}\rangle$ is known only at the N_t sampling points of the time grid. As a simpler alternative the function $|\Phi^{(j)}\rangle$ is expanded in a Taylor series in the time interval $[0, \Delta t]$. Then the coefficients $|\Phi^{(j)}\rangle$ become the j th derivative of $|\Phi(t)\rangle$, at the beginning of the interval. At this point we use the properties of the global N_t interpolation function of $|\Phi(t)\rangle$ to calculate $|\Phi^{(j)}\rangle$ as numerical derivatives at the beginning of each interval.

Based on Eq. (5), the solution of Eq. (3) can be written as

$$|\psi(t)\rangle_{(m)} = \sum_{j=0}^{m-1} \frac{t^j}{j!} |\lambda^{(j)}\rangle + \hat{\mathbf{F}}_m |\lambda^{(m)}\rangle. \quad (6)$$

In Eq. (6), the subscript m denotes the order of the solution. The $|\lambda^{(j)}\rangle$ are obtained iteratively,

$$\begin{aligned} |\lambda^{(0)}\rangle &= |\psi_0\rangle, \\ |\lambda^{(j)}\rangle &= -i\hat{\mathbf{H}}|\lambda^{(j-1)}\rangle + |\Phi^{(j-1)}\rangle, \\ 1 &\leq j \leq m, \end{aligned} \quad (7)$$

and $\hat{\mathbf{F}}_m$ is a function of $\hat{\mathbf{H}}$ and is given by

$$\hat{\mathbf{F}}_m = f_m(\hat{\mathbf{H}}) = (-i\hat{\mathbf{H}})^{-m} \left(e^{-i\hat{\mathbf{H}}t} - \sum_{j=0}^{m-1} \frac{(-i\hat{\mathbf{H}}t)^j}{j!} \right). \quad (8)$$

Equations (6)-(8) represent the formal solution to the inhomogeneous Schrödinger equation.

In order to verify that Eq. (6) is indeed a solution to Eq. (3), let's take the derivative of Eq. (6),

$$\begin{aligned}\frac{\partial}{\partial t}|\psi(t)\rangle_{(m)} &= \sum_{j=0}^{m-1} j \frac{t^{j-1}}{j!} |\lambda^{(j)}\rangle + (-i\hat{\mathbf{H}})^{-m} \left((-i\hat{\mathbf{H}})e^{-i\hat{\mathbf{H}}t} - \sum_{j=1}^{m-1} j(-i\hat{\mathbf{H}}) \frac{(-i\hat{\mathbf{H}}t)^{j-1}}{j(j-1)!} \right) |\lambda^{(m)}\rangle \\ &= \sum_{j=0}^{m-2} \frac{t^j}{j!} |\lambda^{(j+1)}\rangle + (-i\hat{\mathbf{H}})(-i\hat{\mathbf{H}})^{-m} \left(e^{-i\hat{\mathbf{H}}t} - \sum_{j=0}^{m-2} \frac{(-i\hat{\mathbf{H}}t)^j}{j!} \right) |\lambda^{(m)}\rangle.\end{aligned}$$

Inserting Eq. (7) in the first term and resumming with an upper limit $m-1$, one obtains

$$\begin{aligned}\frac{\partial}{\partial t}|\psi(t)\rangle_{(m)} &= \sum_{j=0}^{m-1} \frac{t^j}{j!} \left(-i\hat{\mathbf{H}}|\lambda^{(j)}\rangle + |\Phi^{(j)}\rangle \right) - \frac{t^{m-1}}{(m-1)!} \left(-i\hat{\mathbf{H}}|\lambda^{(m-1)}\rangle + |\Phi^{(m-1)}\rangle \right) \\ &\quad -i\hat{\mathbf{H}}(-i\hat{\mathbf{H}})^{-m} \left(e^{-i\hat{\mathbf{H}}t} - \sum_{j=0}^{m-1} \frac{(-i\hat{\mathbf{H}}t)^j}{j!} + \frac{(-i\hat{\mathbf{H}}t)^{m-1}}{(m-1)!} \right) |\lambda^{(m)}\rangle.\end{aligned}$$

Recognizing $\hat{\mathbf{F}}_m$, cf. Eq. (8), as part of the last term and inserting $|\lambda^{(j)}\rangle$, cf. Eq. (7), in the second term, which then cancels with the second summand of the last term, this can be rewritten

$$\begin{aligned}\frac{\partial}{\partial t}|\psi(t)\rangle_{(m)} &= -i\hat{\mathbf{H}} \left(\sum_{j=0}^{m-1} \frac{t^j}{j!} |\lambda^{(j)}\rangle + \hat{\mathbf{F}}_m |\lambda^{(m)}\rangle \right) \\ &\quad + \sum_{j=0}^{m-1} \frac{t^j}{j!} |\Phi^{(j)}\rangle.\end{aligned}$$

The expression in parenthesis corresponds to $|\psi(t)\rangle$, cf. Eq. (6). Finally, replacing the second term by $|\Phi(t)\rangle$, cf. Eq. (5), the inhomogeneous Schrödinger equation, Eq. (3), is obtained. Therefore Eq. (6) presents indeed a solution to Eq. (3).

III. PROPAGATION SCHEMES

The formal solution, Eq. (6), is subjected to a spectral approximation,

$$|\psi(t)\rangle_{(m)N} = \sum_{j=0}^{m-1} \frac{t^j}{j!} |\lambda^{(j)}\rangle + P_{N(m)}(\hat{\mathbf{H}}) |\lambda^{(m)}\rangle, \quad (9)$$

where P_N is a polynomial of order N approximating $\hat{\mathbf{F}}_m = f_m(\hat{\mathbf{H}})$. For example, to first order, $m = 1$, the formal solution is given by

$$|\psi(t)\rangle_{(1)} = e^{-i\hat{\mathbf{H}}t}|\psi_0\rangle + (-i\hat{\mathbf{H}})^{-1}(e^{-i\hat{\mathbf{H}}t} - \mathbb{1})|\Phi_0\rangle. \quad (10)$$

In principle one might seek a spectral approximation for each of the terms. However, it is numerically more efficient to rewrite the first order solution,

$$|\psi(t)\rangle_{(1)} = |\psi_0\rangle + f_1(\hat{\mathbf{H}}) \left(-i\hat{\mathbf{H}}|\psi_0\rangle + |\Phi_0\rangle \right), \quad (11)$$

with $f_1(\hat{\mathbf{H}}) = (-i\hat{\mathbf{H}})^{-1}(e^{-i\hat{\mathbf{H}}t} - \mathbb{1})$, such that only a single Chebychev expansion plus one extra application of the Hamiltonian are required. Similarly, to second and third order the formal solutions can be written

$$|\psi(t)\rangle_{(2)} = |\psi_0\rangle + t|\lambda^{(1)}\rangle + f_2(\hat{\mathbf{H}})|\lambda^{(2)}\rangle, \quad (12)$$

$$\begin{aligned} |\psi(t)\rangle_{(3)} = |\psi_0\rangle + t|\lambda^{(1)}\rangle + \frac{t^2}{2}|\lambda^{(2)}\rangle \\ + f_3(\hat{\mathbf{H}})|\lambda^{(3)}\rangle \end{aligned} \quad (13)$$

with $f_2(\hat{\mathbf{H}})$ and $f_3(\hat{\mathbf{H}})$ given by Eq. (8) and $|\lambda^{(j)}\rangle$ by Eq. (7). The strategy is then to seek a polynomial approximation for the functions $f_i(\hat{\mathbf{H}})$. For $f_0(\hat{\mathbf{H}}) = e^{-i\hat{\mathbf{H}}t}$, this corresponds to the standard Chebychev propagator for the homogeneous Schrödinger equation [14]. It will be briefly reviewed for clarity, followed by a discussion of the polynomial approximation of the new functions.

A. General idea of the Chebychev propagator

The Chebychev propagator is based on treating the formal solution as a function of an operator which is applied to some state vector,

$$|\phi\rangle = f(\hat{\mathbf{H}})|\psi\rangle,$$

and to approximate this function by an expansion in Chebychev polynomials P_n ,

$$f(\hat{\mathbf{H}})|\psi\rangle = \sum_n a_n P_n(\hat{\mathbf{H}})|\psi\rangle.$$

Since the Chebychev polynomials are defined within the range $[-1, 1]$, the Hamiltonian has to be renormalized,

$$\hat{\mathbf{H}}_{norm} = 2 \frac{\hat{\mathbf{H}} - E_{min}\mathbb{1}}{\Delta E} - \mathbb{1},$$

where E_{min} denotes the smallest eigenvalue of $\hat{\mathbf{H}}$ and $\Delta E = E_{max} - E_{min}$ the spectral range of $\hat{\mathbf{H}}$. The wavefunction propagated from $t = 0$ to time t is then obtained by

$$|\psi(t)\rangle \cong e^{-i(\frac{1}{2}\Delta E + E_{min})t} \sum_{n=0}^N a_n P_n(-i\hat{\mathbf{H}}_{norm})|\psi_0\rangle,$$

where the phase factor in front of the sum is due to the renormalization.

The algorithm to estimate $|\phi\rangle = f(\hat{\mathbf{H}})|\psi\rangle$ proceeds as follows:

1. Calculate the expansion coefficients a_n ,

$$a_n = \frac{2 - \delta_n}{\pi} \int_{-1}^1 \frac{f(x)P_n(x)}{\sqrt{1-x^2}} dx. \quad (14)$$

For the function $f(x) = f_0(x) = e^{-ixt}$, the integrals can be solved analytically resulting in the Bessel functions [14].

2. Calculate $P_n(-i\hat{\mathbf{H}}_{norm})|\psi_0\rangle$ using the recursion relation of the Chebychev polynomials,

$$\begin{aligned} |\phi_0\rangle &= |\psi_0\rangle, \\ |\phi_1\rangle &= -i\hat{\mathbf{H}}_{norm}|\psi_0\rangle, \\ |\phi_n\rangle &= -2i\hat{\mathbf{H}}_{norm}|\phi_{n-1}\rangle + |\phi_{n-2}\rangle. \end{aligned}$$

3. Accumulate the result, taking into account the phasefactor due to renormalization,

$$|\psi(t)\rangle = e^{-i(\frac{1}{2}\Delta E + E_{min})t} \sum_{n=0}^N a_n |\phi_n\rangle.$$

Task 1 has to be performed only once, while 2 and 3 are repeated for each propagation step. The number N of Chebychev polynomials is chosen such that the coefficient a_{N+1} becomes smaller than some specified error ε . Since the coefficients can be determined analytically, ε may correspond to the machine precision of the computer.

B. Chebychev propagator for inhomogeneous equations

According to Eqs. (10-13) a single Chebychev expansion plus a few applications of the Hamiltonian are required to solve the inhomogeneous Schrödinger equation. In particular, the application of a function $f_m(\hat{\mathbf{H}})$ to a state vector $|\lambda^{(m)}\rangle$ has to be considered,

$$|\phi\rangle = f_m(\hat{\mathbf{H}})|\lambda^{(m)}\rangle, \quad (15)$$

where $|\lambda^{(m)}\rangle$ is simply a 'state vector' obtained recursively by Eq. (7). The Chebychev propagation scheme now consists in calculating $|\lambda^{(m)}\rangle$ and performing tasks 1–3 for $f_m(\hat{\mathbf{H}})|\lambda^{(m)}\rangle$.

There are two differences between the standard Chebychev propagator, i.e. approximation of $f_0(\hat{\mathbf{H}})$, and approximation of $f_{m>0}(\hat{\mathbf{H}})$. (i) For $m > 0$, the integrals required to calculate the expansion coefficients a_n , Eq. (14), cannot be solved analytically anymore. They can, however, be obtained numerically with sufficient efficiency and accuracy. Since the Chebychev polynomials can be expressed in terms of cosines, Eq. (14) can be viewed as a cosine transformation [15]. The expansion coefficients can thus be evaluated by Fast Cosine Transformation. Special care is, however, required for small values of the argument of $f_m(\hat{\mathbf{H}})$ since $f_m(\hat{\mathbf{H}})$ involves division by the m th power of $\hat{\mathbf{H}}$. It is recommended to employ the definition of $f_m(\hat{\mathbf{H}})$, Eq. (8), only if the argument is larger than some small value ϵ and to use a Taylor expansion of $f_m(\hat{\mathbf{H}})$,

$$f_{m>0}(\hat{\mathbf{H}}) = t^m \sum_{j=0}^{\infty} \frac{(-i\hat{\mathbf{H}}t)^j}{(j+m)!} \quad (16)$$

for arguments smaller than ϵ .

(ii) As explained in Section II we use a Taylor expansion of $|\Phi(t)\rangle$ for each integration interval. Recursive calculation of $|\lambda^{(m)}\rangle$ then requires numerical evaluation of the time derivatives of the 'inhomogenous state vector', $|\Phi(t)\rangle$. Second order $m = 2$ requires the first derivative which can be obtained with sufficient accuracy by Fast Fourier Transformation (FFT) and multiplication in frequency domain. However, an error is introduced due to finite values of $|\Phi(t)\rangle$ at the boundaries of the grid, i.e. $t = 0$ and $t = T$. This error is increased and propagated throughout the time interval in the calculation of higher order derivatives by FFT and multiplication in frequency domain. Higher order schemes require therefore a different method for the evaluation of the derivatives. We choose to represent $|\Phi(t)\rangle$ by an expansion into Chebychev polynomials. The derivatives are then calculated recursively based on the analytical properties of the Chebychev polynomials [16]. Note that this implies a non-equidistant time grid since the roots of the Chebychev polynomials need to be taken as sampling points,

$$t'_n = \cos\left(\frac{n\pi}{N_t - 1}\right), \quad t_n = \frac{T}{2} \left(1 + \cos\left(\frac{n\pi}{N_t - 1}\right)\right) \\ n = 0, \dots, N_t - 1,$$

where the time interval $t \in [0, T]$ is scaled to $t' \in [-1, 1]$ and N_t denotes the number

of sampling points. A non-equidistant time grid requires calculation and storage of the Chebychev expansion coefficients of the propagator for each Δt_n . This additional effort is well paid off since a higher order scheme allows for larger time steps, i.e. smaller N_t .

C. Approximation of the formal solution by Taylor expansion

As shown in Appendix A, the formal solution, Eq. (6), can also be written as

$$|\psi(t)\rangle_{(m)} = e^{-i\hat{\mathbf{H}}t}|\psi_0\rangle + \sum_{j=0}^{m-1} \hat{\mathbf{F}}_{j+1} |\Phi^{(j)}\rangle, \quad (17)$$

with

$$\hat{\mathbf{F}}_{j+1} = (-i\hat{\mathbf{H}})^{-(j+1)} \left(e^{-i\hat{\mathbf{H}}t} - \sum_{k=0}^j \frac{(-i\hat{\mathbf{H}}t)^k}{k!} \right).$$

Taking the Taylor expansion of the exponential in $\hat{\mathbf{F}}_{j+1}$ up to order $j+1$,

$$e^{-i\hat{\mathbf{H}}t} = \sum_{k=0}^{j+1} \frac{(-i\hat{\mathbf{H}}t)^k}{k!} = \sum_{k=0}^j \frac{(-i\hat{\mathbf{H}}t)^k}{k!} + \frac{(-i\hat{\mathbf{H}}t)^{j+1}}{(j+1)!},$$

one obtains an approximation of Eq. (17),

$$|\psi(t)\rangle_{(m)} = e^{-i\hat{\mathbf{H}}t}|\psi_0\rangle + \sum_{j=0}^{m-1} \frac{t^{j+1}}{(j+1)!} |\Phi^{(j)}\rangle. \quad (18)$$

This approximation can be used to simplify the numerical implementation of the algorithm. To all orders, only the standard Chebychev propagation scheme plus calculation and storage of the derivatives of the inhomogeneous term are required. For example, the approximate solution to second order reads

$$|\psi(t)\rangle_{(2)} \approx f_0(\hat{\mathbf{H}})|\psi_0\rangle + t|\Phi^{(0)}\rangle + \frac{t^2}{2}|\Phi^{(1)}\rangle. \quad (19)$$

Unlike the propagator described in Section IIIB, this scheme is explicitly based on a Taylor expansion, so we expect it to be valid only for small time steps. In that case, a low order scheme (e.g. $m=2$) is sufficient. The necessary derivatives can then be calculated by FFT and multiplication in frequency domain. The validity of this approximation is discussed in detail in Section IVB.

IV. APPLICATION I: CONTROL WITH A STATE-DEPENDENT CONSTRAINT

In our first example, the operator occurring in the inhomogeneous term is not time-dependent, $\hat{\mathbf{G}}(t) = \hat{\mathbf{G}}$.

A. Model

A simplified model of the vibrations in a Rb_2 molecule is considered taking into account three electronic states [7]. The corresponding Hamiltonian reads

$$\hat{\mathbf{H}} = \sum_{i=1}^3 \hat{\mathbf{H}}_i \otimes |e_i\rangle\langle e_i| + \hat{\boldsymbol{\mu}} \epsilon(t) \cdot \left(|e_1\rangle\langle e_2| + |e_2\rangle\langle e_1| + |e_2\rangle\langle e_3| + |e_3\rangle\langle e_2| \right), \quad (20)$$

where $\hat{\mathbf{H}}_i$ denotes the vibrational Hamiltonians, $\hat{\mathbf{H}}_i = \hat{\mathbf{T}} + V_i(\hat{\mathbf{R}})$, $\hat{\boldsymbol{\mu}}$ the transition dipole operator, assumed to be independent of $\hat{\mathbf{R}}$, and $\epsilon(t)$ the electric field. The electronic states are associated to $X^1\Sigma_g^+(5s + 5s)$, $^1\Sigma_u^+(5s + 5p)$ and $^1\Pi_g(5s + 4d)$, with the potentials found in Ref. [17].

OCT shall be employed to transfer population from the vibrational ground state of the electronic ground surface to some vibrationally excited state via Raman transitions between the ground and the second electronic surface. For strong laser fields $\epsilon(t)$, such as those found by OCT algorithms, population at intermediate times will be excited not only to the second but also to the third electronic surface. This is particularly the case for the electronic states of our example, where transition frequencies and Franck-Condon factors for transitions between $|e_1\rangle$ and $|e_2\rangle$ are very similar to those for transitions between $|e_2\rangle$ and $|e_3\rangle$. Assuming that the third electronic state corresponds to a loss channel, e.g. an intermediate state in resonantly enhanced multi-photon ionization or an autoionizing state, population transfer into this state should be avoided at all times. This can be communicated to the OCT algorithm by formulating a state-dependent constraint which maximizes the projection onto the allowed subspace [7], i.e. onto electronic states 1 and 2. The complete functional for optimization is then given by [7]

$$J[\varphi, \varphi^*, \epsilon] = J_0[\varphi_T, \varphi_T^*] + J_a[\epsilon] + J_b[\varphi, \varphi^*] \quad (21)$$

with

$$J_0[\varphi_T, \varphi_T^*] = \lambda_0 \langle \varphi(T) | \hat{\mathbf{D}} | \varphi(T) \rangle, \quad (22)$$

$$J_a[\epsilon] = \int_0^T \lambda_a(t) [\epsilon(t) - \epsilon_r(t)]^2 dt, \quad (23)$$

$$J_b[\varphi, \varphi^\dagger] = \int_0^T \lambda_b \langle \varphi(t) | \hat{\mathbf{P}}_{\text{allow}} | \varphi(t) \rangle dt. \quad (24)$$

The operator $\hat{\mathbf{D}}$ in J_0 is given by the projector onto the target level in the electronic ground state. The state-dependent constraint contains the projector onto the allowed subspace, $\hat{\mathbf{P}}_{\text{allow}}$. In Ref. [7], propagation via full diagonalization of the Hamiltonian was employed and only 11 vibrational levels in each electronic state were considered. Representing the vibrational Hamiltonians on a Fourier grid [12] and utilizing the inhomogeneous Chebychev propagator, the full potentials can be taken into account ($N_{\text{grid}} = 128$).

B. Test of the propagator

In order to test the new Chebychev propagator, our numerical results are compared to those obtained by the symmetrical method for the Hamiltonian comprising of 11 levels in each electronic state [7]. The inhomogeneous Schrödinger equation reads [7]

$$\frac{d}{dt} |\psi(t)\rangle = -\frac{i}{\hbar} \hat{\mathbf{H}}[\epsilon(t)] |\psi(t)\rangle + \lambda_b \hat{\mathbf{P}}_{\text{allow}} |\varphi(t)\rangle, \quad (25)$$

with the “initial” condition

$$|\psi(t=T)\rangle = -\lambda_0 \hat{\mathbf{D}} |\varphi(T)\rangle. \quad (26)$$

In OCT, $|\psi(t)\rangle$ is the backward propagated wavefunction which is coupled to $|\varphi(t)\rangle$ obtained by forward propagation,

$$\frac{d}{dt} |\varphi(t)\rangle = -\frac{i}{\hbar} \hat{\mathbf{H}}[\epsilon(t)] |\varphi(t)\rangle \quad (27)$$

with $|\varphi(t=0)\rangle = |\varphi_0\rangle$. The convergence with respect to the time step Δt and the order m of the Chebychev method will be discussed in Section IV C.

We start by propagating the initial state, $v = 0$ of the electronic ground state, forward with a Gaussian pulse given by Eq. (33) of Ref. [7]. The inhomogeneous Schrödinger equation is then propagated backward with the same field. All parameters are taken to be equal to those of Ref. [7]. Figure 1 shows the expectation value of the projector onto the

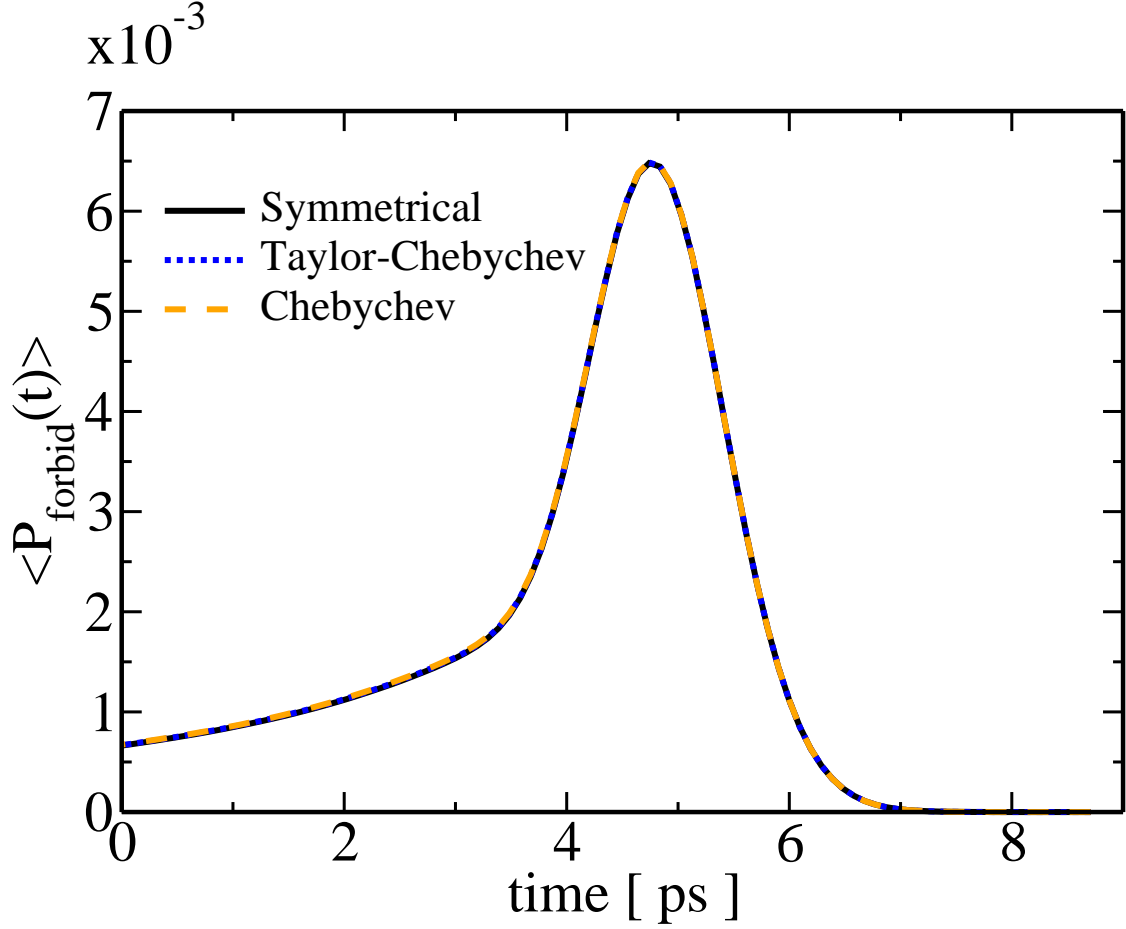


FIG. 1: (color online) Normalized expectation value of the projector onto the forbidden subspace for a single backward propagation with a Gaussian pulse. Comparison between the symmetrical scheme of Ref. [7] with $\Delta t = 1$ a.u. (black solid line), the Chebychev propagator in first order with $\Delta t = 1$ a.u. (orange dashed line) and the Chebychev propagator in first order based on the Taylor approximation, Eq.(18), with $\Delta t = 0.1$ a.u. (blue dotted line).

forbidden subspace, $\langle \hat{\mathbf{P}}_{\text{forbid}} \rangle(t)$, for normalized $|\psi(t)\rangle$. Results for the symmetrical method and the first order Chebychev propagators based on Eq. (6) and on Eq. (18) (Taylor) are compared. A good agreement between the Chebychev propagators and the symmetrical scheme is found. The time step needed to obtain converged results with the approximate solution is, however, smaller by a factor of ten. This is not surprising since the approximate solution is based on a Taylor expansion which requires a very small Δt .

Our main motivation for the development of the modified Chebychev propagator lies in its application in OCT with a state-dependent constraint or a time-dependent target. There-

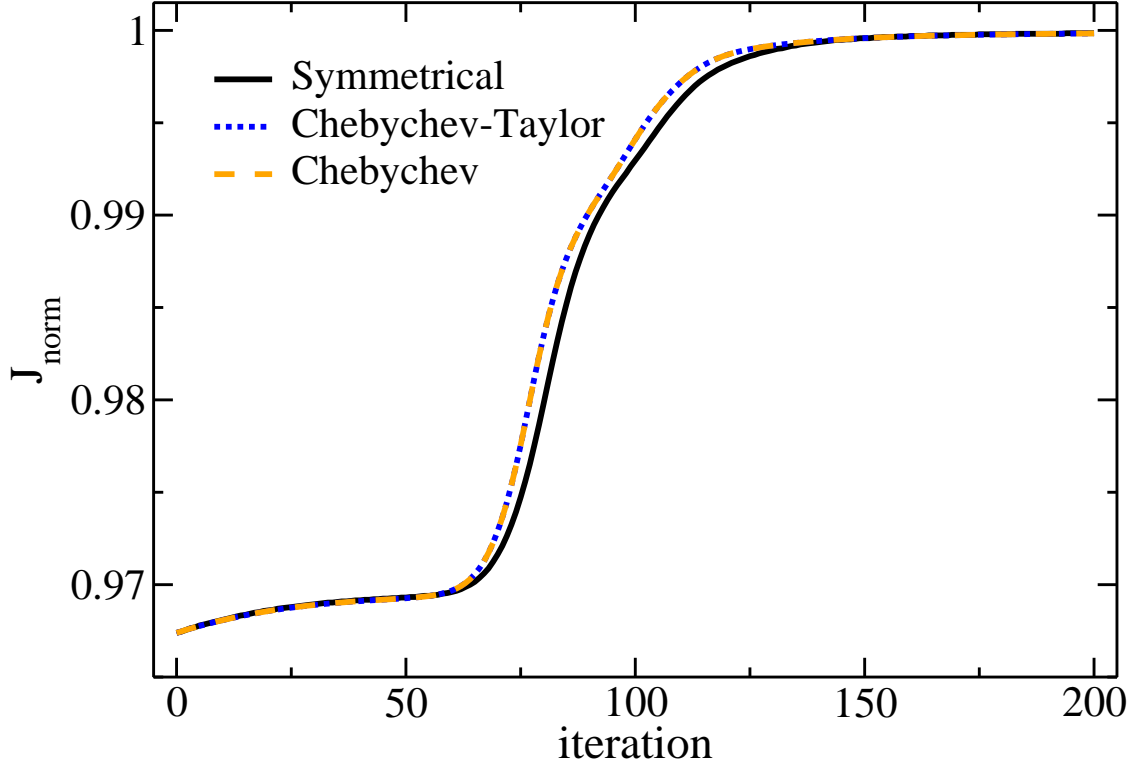


FIG. 2: (color online) J_{norm} as a function of the number of iterations. Solution obtained by the symmetrical scheme of Ref. [7] with a time step $\Delta t = 1$ a.u. (black solid line), the Chebychev propagator for first order with a time step $\Delta t = 1$ a.u. (orange dashed line) and the second order approximate solution of Eq.(18) with a time step $\Delta t = 0.1$ a.u. (blue dotted line).

fore the new propagator is also tested in an iterative solution of the control equations. The control problem is that of Ref. [7]. However, in the present work the full vibrational Hamiltonians are employed. Convergence of the OCT algorithm is measured by the normalized functional, $J_{\text{norm}} = J/(\lambda_0 + \lambda_b T)$, approaching one as the control equations are iteratively solved, cf. Fig. 2. The symmetrical scheme ($\Delta t = 1$ a.u., black solid line) is compared to the Chebychev propagator in first order (orange dashed line) and to the Chebychev propagator based on the Taylor approximation, Eq. (18), (blue dotted line) in second order. An overall good agreement is found. The difference between the results at intermediate iterations is attributed to the different models, the full vibrational Hamiltonian in the case of the Chebychev propagators and the Hamiltonian consisting of 33 levels in the case of the symmetrical method. Application of the Chebychev propagator based on the Taylor approximation, Eq. (18), in first order failed: The inhomogeneous Schrödinger equation is solved

with insufficient accuracy and the property of monotonic convergence of the Krotov method [10] is lost during the iterative solution of the control equations. This is easily rationalized in terms of the very fast oscillations occurring in the optimized field. They require either a very small time step or a higher order in the approximation of the exponential, $e^{-i\hat{\mathbf{H}}\Delta t}$, by a Taylor expansion. The complexity of the pulse and hence the time variation of the inhomogeneous term determine the required order of the Taylor approximation.

C. Convergence behavior

The convergence and the efficiency of the inhomogeneous Chebychev propagator are analyzed with respect to the number of time steps N_t and the order m of the solution. The main numerical effort is required for the application of the Hamiltonian and the calculation of the derivatives. For a given propagation time T one would like to identify optimum values of N_t and m that yield a minimum computation time for a specified accuracy. In general, decreasing the number of time steps N_t or, respectively, increasing Δt will require a larger number of Chebychev polynomials in the expansion of the function $f_m(\hat{\mathbf{H}})$, but also a higher order m of the solution. The recursive calculation of the Chebychev polynomials in the expansion of $f_m(\hat{\mathbf{H}})$ implies continued application of the Hamiltonian. Moreover, higher order solutions require additional applications of the Hamiltonian, cf. Eqs. (10-13), and determination of derivatives of the inhomogeneous term up to degree $m - 1$.

We consider first equidistant time steps and evaluate the time derivatives by FFT. Figure 3 traces the population in the forbidden subspace to illustrate the convergence behavior for dynamics under a Gaussian pulse. In first order, cf. Fig. 3a, the dynamics are found to be converged for time steps $\Delta t \leq 2$ a.u. At larger time steps, deviations are observed, in particular at short times (occurring late for backward propagation). Dynamics with the largest possible time step at each order are shown in Fig. 3b. In order to decide whether it is numerically more efficient to keep a low order demanding a small time step or to employ a higher order allowing for a larger time step, Table I compares the CPU time required to obtain converged solutions in first, second and third order. The number of applications of $\hat{\mathbf{H}}$ includes both those occurring in the Chebychev recursion and those due to the additional terms in Eqs. (10-13). For example, for third order and $\Delta t = 6$ a.u., 10 Chebychev polynomials are sufficient to approximate $f_3(\hat{\mathbf{H}})$ Eq. (13). Each time step

order m	Δt	N_t	N_{Cheby}	applications of $\hat{\mathbf{H}}$	CPU time
1	2 a.u.	180.000	6	1.260.000	12 s
2	4 a.u.	90.000	8	900.000	11 s
3	6 a.u.	60.000	10	780.000	9 s

TABLE I: CPU time required for one backward propagation to obtain converged solutions in first, second and third order for a total propagation time of 8 ps with equidistant time steps Δt . Also listed are the number of time steps, N_t , the number of times the Hamiltonian is applied and the number of terms in the Chebychev expansion, N_{Cheby} .

then implies thirteen applications of $\hat{\mathbf{H}}$, ten for the Chebychev recursion plus three for the additional terms (one for $|\lambda^{(1)}\rangle$ and two for $|\lambda^{(2)}\rangle$), cf. Eqs. (13) and (7). As can be seen in Table I, in terms of CPU time, it is more efficient to employ a higher order solution. In the context of OCT calculations, in addition to saving computation time, a higher order propagator also allows for saving memory since the backward propagated wavefunction needs to be stored for each time step. An inherent limit to increasing the time step is, however, posed by the time-dependence of the Hamiltonian. Expressing the formal solution of the homogeneous time-dependent Schrödinger equation by the exponential, $e^{-i\hat{\mathbf{H}}\Delta t}$, assumes $\hat{\mathbf{H}}$ to be constant within the time interval Δt . In our example the upper limit at third order, $\Delta t = 6$ a.u., is due to the breakdown of this assumption for the forward propagated wavefunction, $|\varphi(t)\rangle$, entering the inhomogeneous term, $\lambda_b \hat{\mathbf{P}}_{\text{allow}} |\varphi(t)\rangle$.

In order to demonstrate that a higher-order solution for the inhomogeneous Schrödinger equation allows indeed for a large time step, we modify our example by invoking the rotating-wave approximation (RWA). This eliminates highly oscillatory terms from the field, $\epsilon(t)$, keeping only the time-dependence of the envelope which is several orders of magnitude slower. However, when increasing the time step and the order, numerical determination of the derivatives by FFT and multiplication in frequency domain breaks down, cf. Section III B. Accurate numerical calculation of the time derivatives of the inhomogeneous term, $|\Phi(t)\rangle = \lambda_b \hat{\mathbf{P}}_{\text{allow}} |\varphi(t)\rangle$, is afforded by expanding $|\Phi(t)\rangle$ in Chebychev polynomials. The sampling points of the time grid then need to be chosen as the roots of the Chebychev polynomials, leading to non-equidistant time steps (dividing the time interval into equidistant time steps corresponds to a Fourier representation). Figure 4 and Table II illustrate the convergence

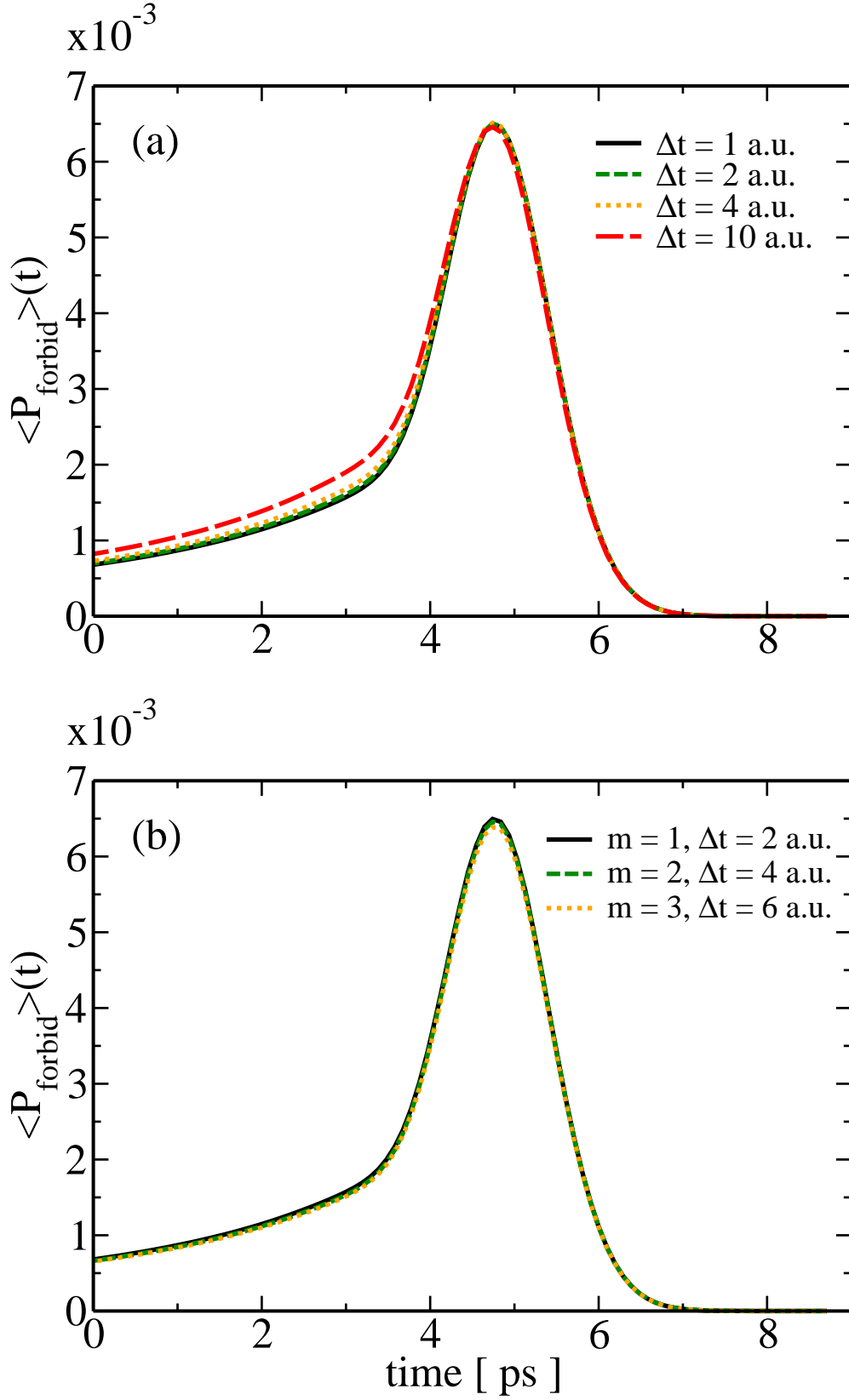


FIG. 3: (color online) Normalized expectation value for the projector onto the forbidden subspace demonstrating the convergence of the inhomogeneous Chebychev propagator: (a) for first order solutions ($m = 1$), convergence is lost by increasing Δt , (b) converged results for the largest possible time step at a given order m .

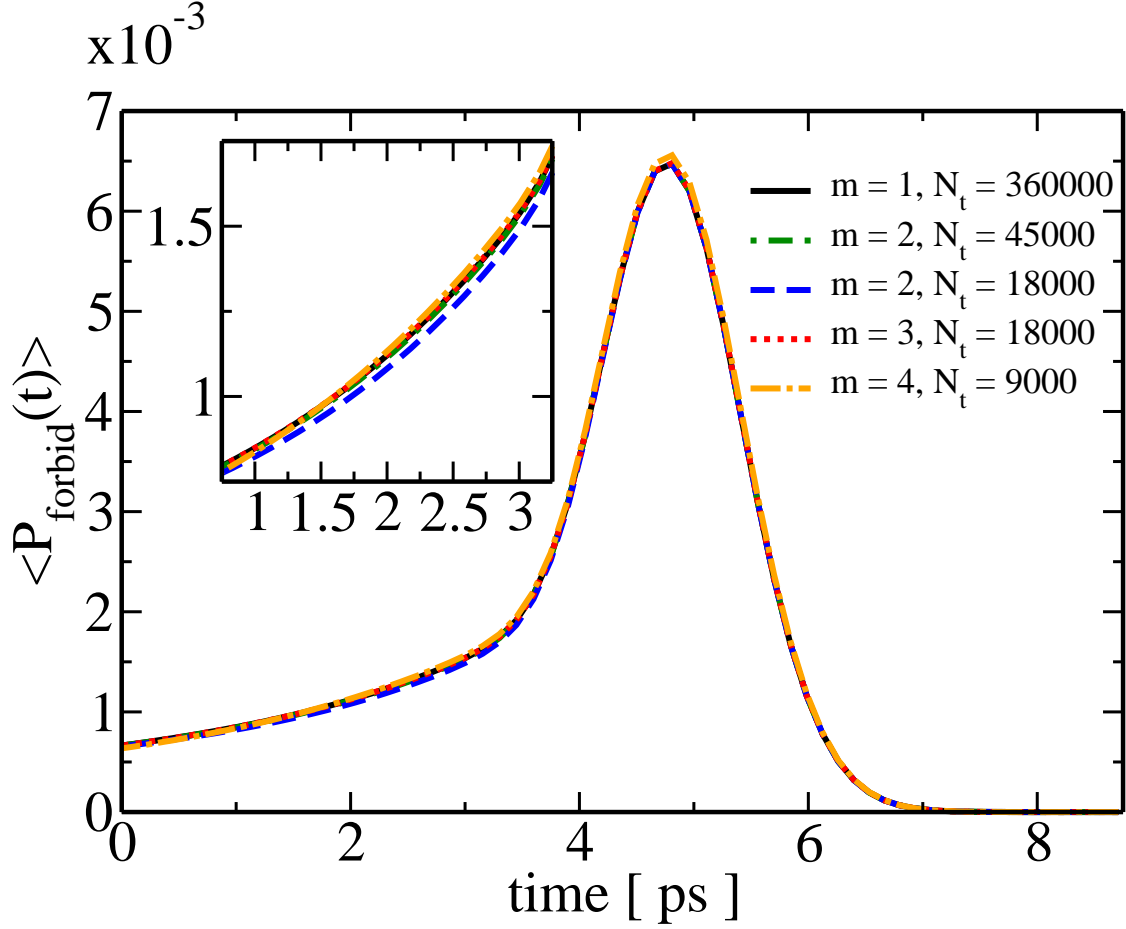


FIG. 4: (color online) Normalized expectation value of the projector onto the forbidden subspace for a Hamiltonian with slow time-dependence (RWA) employing a non-equidistant time grid and calculating time derivatives in terms of Chebychev expansions for different orders m . Results are shown for the smallest possible number of time steps, N_t , at given order m except for $m = 2$, $N_t = 18000$ (blue dashed line) which illustrates a non-converged case.

behavior for a Hamiltonian with slow time-dependence. All results in Fig. 4 are shown for the smallest possible number of time steps except the blue dashed line ($m = 2$, $N_t = 18.000$) which illustrates a non-converged case, cf. the deviation from the converged results at short times. The number of time steps can be significantly reduced by employing higher-order schemes. The evaluation of the derivatives by Chebychev expansion is, however, more costly, leading to overall larger computation times than in Table I. It is obvious from Table II that this variant of the inhomogeneous Chebychev propagator will unfold its full power for a time-independent Hamiltonian that occurs e.g. in reactive scattering calculations where a very

order m	N_t	Δt_{\max}	CPU time
2	45.000	12.6 a.u.	170 s
3	18.000	31.4 a.u.	69 s
4	9.000	62.8 a.u.	35 s

TABLE II: CPU time required to obtain converged solutions in second, third and fourth order for a total propagation time of 8 ps with non-equidistant time steps. Also listed are the smallest possible number of sampling points for the time grid, N_t , and the corresponding maximum time step, Δt_{\max} .

large time step together with a high-order scheme will be numerically most efficient. The fact that the permissible time step can be increased by employing a higher-order solution illustrates that inhomogeneous Chebychev propagator is based on a global representation.

V. APPLICATION II: CONTROL WITH A TIME-DEPENDENT TARGET

In our second application, the operator occurring in the inhomogeneous term, $\hat{\mathbf{G}}(t)$, is explicitly time-dependent.

A. Model

In principle it should be possible to prescribe by a laser pulse an arbitrary pathway that the quantum system should follow. To this end, OCT with a time-dependent target has to be employed [4, 6]. In the total functional, Eq. (21), the final-time term then disappears, $J_0[\varphi_T, \varphi_T^*] = 0$, and the state- and time-dependent term becomes [7]

$$J_b[\varphi, \varphi^\dagger] = \int_0^T \lambda_b \langle \varphi(t) | \hat{\mathbf{G}}(t) | \varphi(t) \rangle dt. \quad (28)$$

Maximization of J_b corresponds to $\lambda_b \geq 0$ and fulfills the conditions for monotonic convergence [7].

A simple model comprising of five of the 33 levels of Section IV are taken to mimic a double Λ -system, cf. Fig. 5. Initially all population is assumed to be in $v = 0$, and at the final time the population in $v = 2$ is to be maximal. Additionally, the time interval $[0, T]$ is divided into subintervals where the population of the intermediate levels $v' = 6$, $v = 1$,

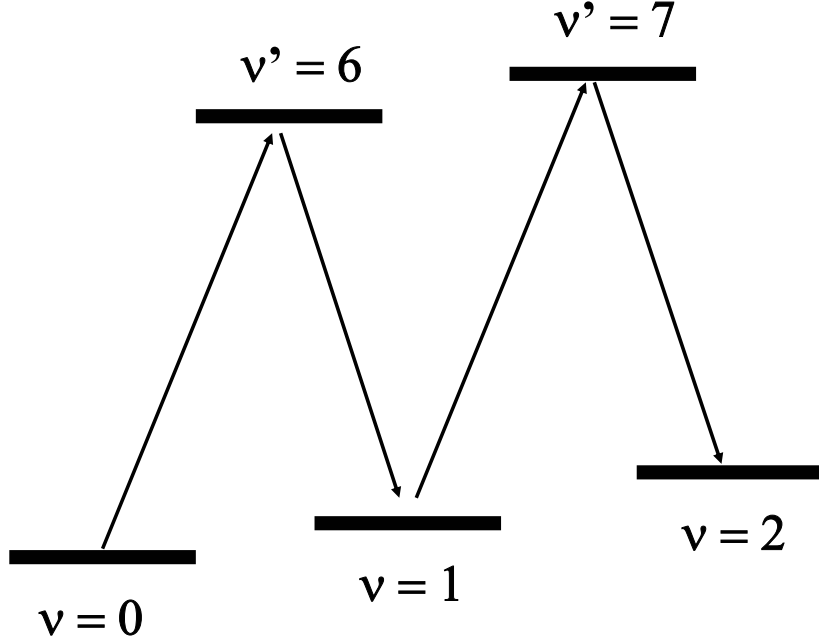


FIG. 5: Prescribed 'trajectory' for a time-dependent target: climbing up the ladder of a double Λ -system.

and $v' = 7$, is maximized, i.e. we prescribe a 'trajectory' where the ladder of the double Λ -system is sequentially climbed up. While this represents a simple toy model, it serves the purpose of illustrating the case where the operator of the inhomogeneous term of the Schrödinger equation, $\hat{\mathbf{G}}(t)$, is explicitly time-dependent. The inhomogeneous equation for backward propagation reads,

$$\frac{d}{dt}|\psi(t)\rangle = -\frac{i}{\hbar}\hat{\mathbf{H}}[\epsilon(t)]|\psi(t)\rangle + \lambda_b\hat{\mathbf{G}}(t)|\varphi(t)\rangle, \quad (29)$$

with the "initial" condition

$$|\psi(t = T)\rangle = 0. \quad (30)$$

Dividing the time interval $[0, T]$ into four subintervals, $0 < T_1 < T_2 < T_3 < T$, the target is defined as the projector onto $v' = 6$ in $[0, T_1]$, onto $v = 1$ in $[T_1, T_2]$, onto $v' = 7$ in $[T_2, T_3]$

and onto $v = 2$ in the subinterval $[T_3, T]$,

$$\begin{aligned}\hat{\mathbf{G}}(t) = & |6\rangle\langle 6|\Theta(T_1 - t) + \\ & |1\rangle\langle 1|\Theta(t - T_1)\Theta(T_2 - t) + \\ & |7\rangle\langle 7|\Theta(t - T_2)\Theta(T_3 - t) \\ & |2\rangle\langle 2|\Theta(t - T_3)\Theta(T - t)\end{aligned}\quad (31)$$

with $\Theta(t)$ the Heaviside function. In order to avoid numerical problems due to discontinuities, $\Theta(t)$ is approximated by

$$\Gamma(t) = \frac{1}{1 + e^{-kt}}, \quad (32)$$

where the parameter k determines the steepness with which the target level changes. While for large values of k , the step function is recovered, small values of k imply overlap in time of two different targets near the T_i , $i = 1 - 3$. In the following k is varied between $k = 10^{-4}$ a.u. and $k = 10^4$ a.u. The final time is set to $T = 5.4$ ps. The subintervals are taken to be of the same length, $T_1 = 1.35$ ps, $T_2 = 2T_1$ and $T_3 = 3T_1$.

B. Results

The new propagator is tested for the iterative solution of the control equations with the time-dependent target. The guess field consists of a sequence of four π -pulses, one in each time interval. Figure 6 shows the evolution of the level populations using the optimized field for $k = 10^4$. They follow by and large indeed the prescribed 'trajectory'. Population of levels other than the target one and fast oscillations in the populations are observed only when switching from one target to the next. The spectrum of the optimized field is shown in Fig. 7. The transition frequencies of our model, listed in Table III and indicated in Fig. 7b, are contained within the spectrum. Additional frequencies which do not correspond to the main transition frequencies are observed. They are attributed to the complexity of the optimal solution which may include beatings between levels, Stark shifts etc.

The improvement of the time-dependent target functional with the number of iterations is demonstrated in Fig. 8 for different values of the steepness parameter k . Monotonic convergence is observed. However, the algorithm cannot reach 100%. We attribute this to the way the target is switched and overlap in time of different targets is created around the T_i , $i = 1 - 3$. For large k the changes in the target functional are almost instantaneous and

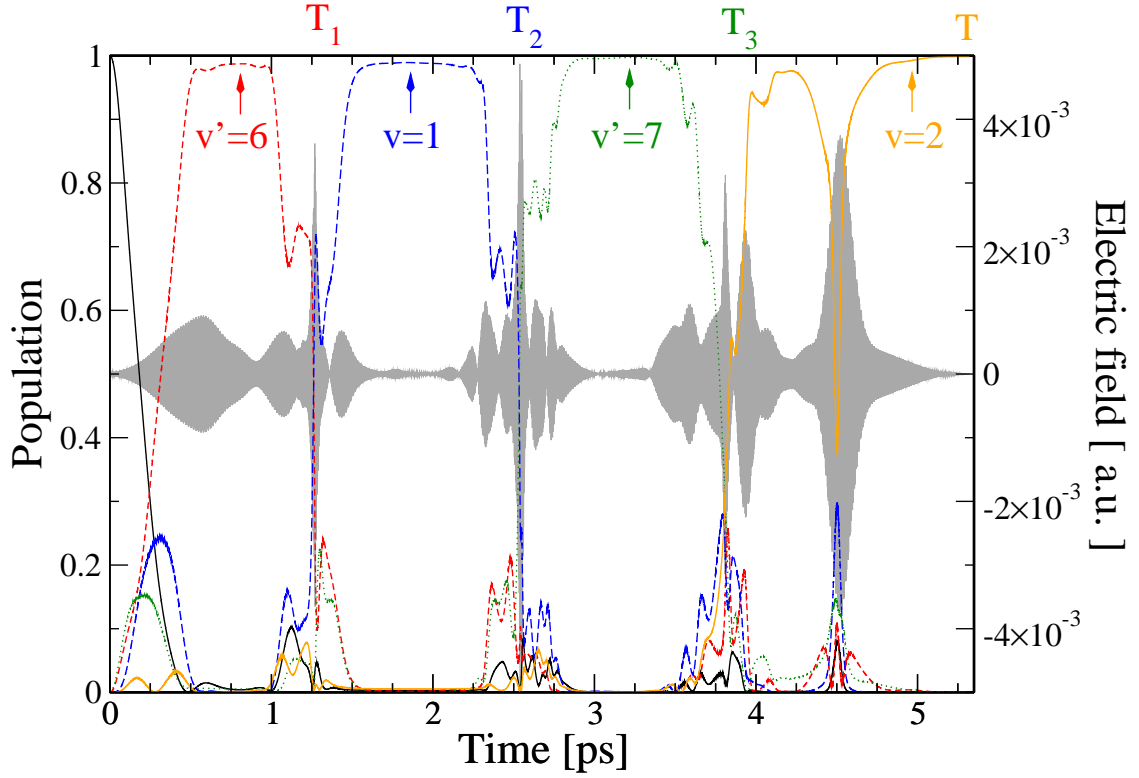


FIG. 6: (color online) Time-dependent target: Time evolution of the level populations with an optimal field (shown in grey).

8

	0	1	2
6	11130	11072	11014
7	11172	11114	11057

TABLE III: Transition frequencies in cm^{-1} for the five levels employed as time-dependent target.

cannot be followed by the dynamics, cf. the oscillations in the level populations in Fig. 6. However, at the same time, the targets do almost not overlap. This yields the highest value of the target functional, about 85%. For smaller values of k the dynamics can follow more smoothly. However, the overlap between different targets is increased, i.e. contradictory objectives are asked at the same time. This decreases the value of the target functional to about 79%.

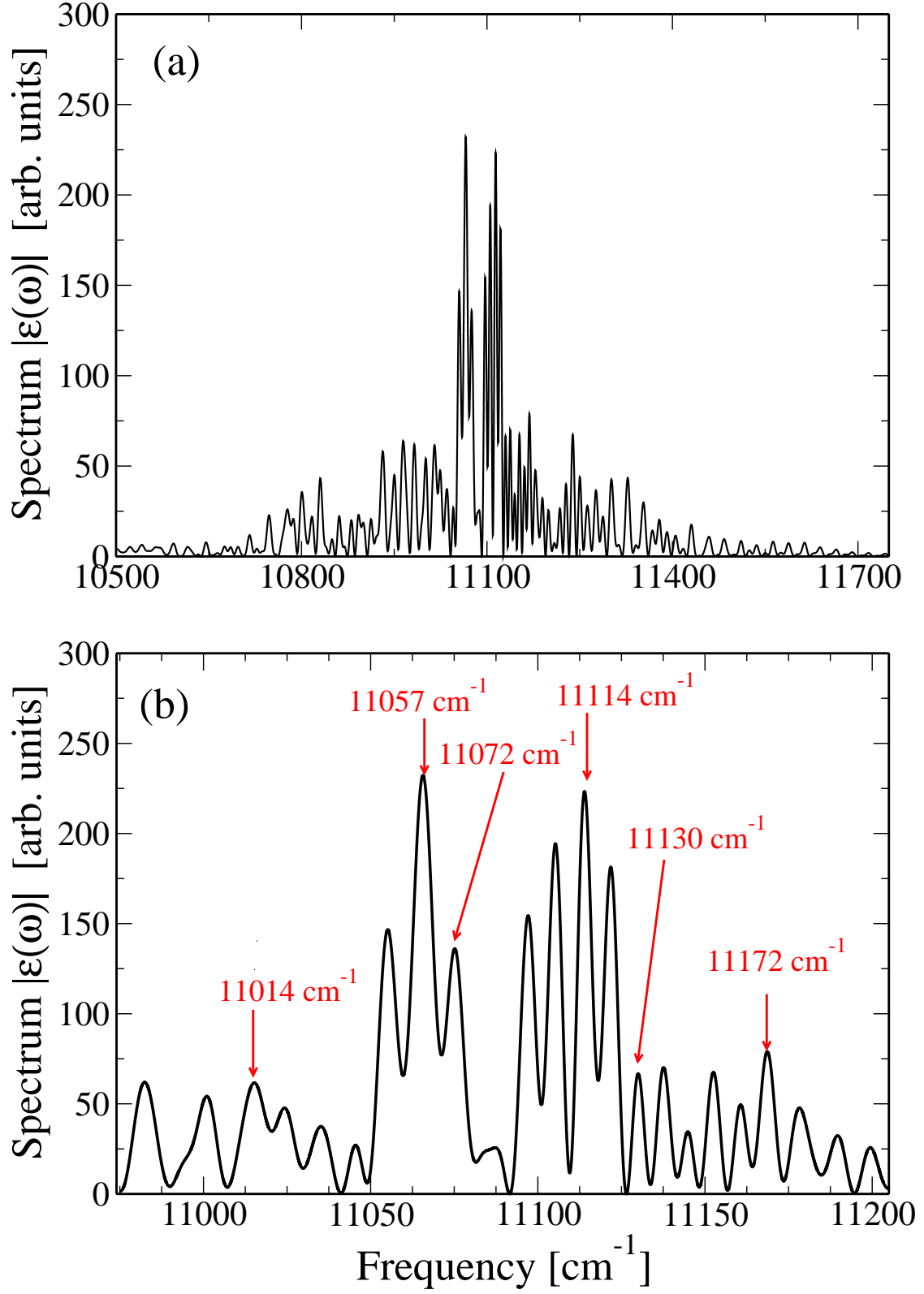


FIG. 7: (color online) (a) Spectrum of the optimized field. (b) Detail of the spectrum ($\omega \in [10975 \text{ cm}^{-1}, 11205 \text{ cm}^{-1}]$). The numbers and arrows indicate the six main transition frequencies of the model, cf. Table III.

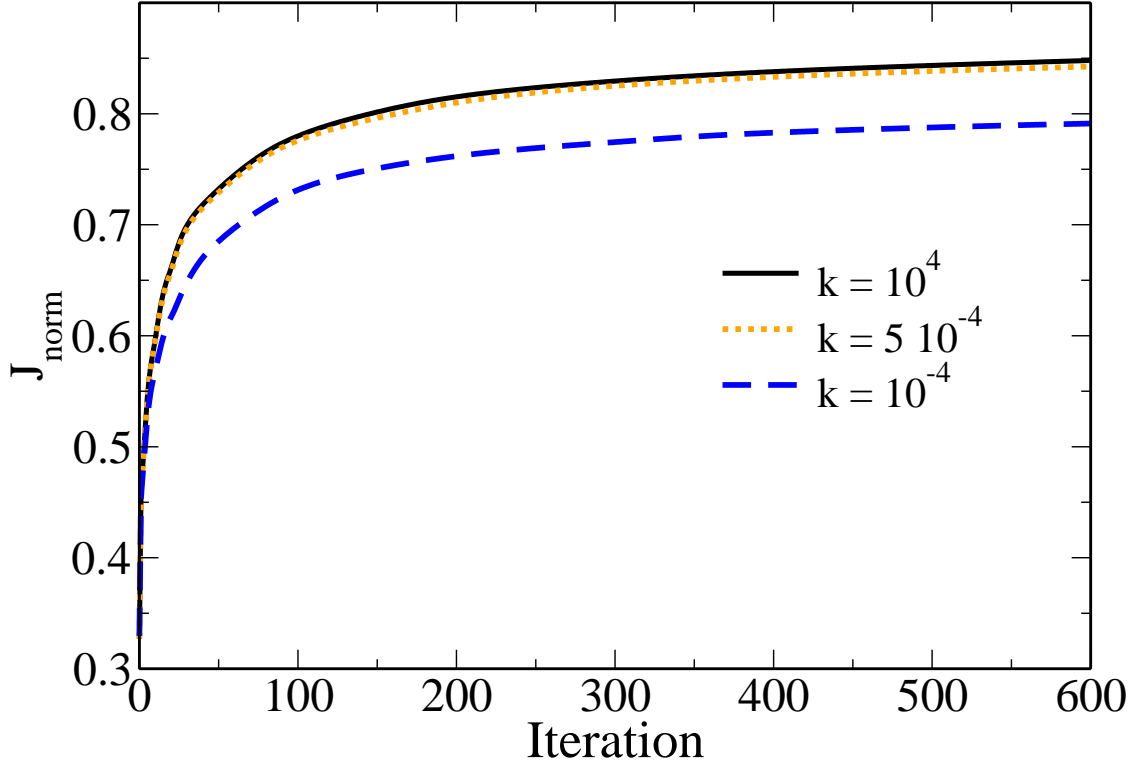


FIG. 8: (color online) The renormalized functional J_b , cf. Eq. (28), as a function of the number of iterations for parameters k corresponding to different overlaps in time of two targets.

C. Convergence behavior

The convergence of the inhomogeneous Chebychev propagator is again analyzed with respect to the time step Δt and to the order m . We restrict ourselves here to the case of equidistant time steps and calculation of the derivatives by FFT and multiplication in frequency domain. The convergence behavior is illustrated in Fig. 9 by the time evolution of the final target level ($v = 2$) population. Converged results are obtained for $\Delta t \leq 4$ a.u. ($\Delta t \leq 10$ a.u.) in first (second) order, i.e. a larger time step than in Section IV can be used. We attribute this to the much simpler model.

Table IV compares the CPU time required to obtain converged solutions in first and second order. The same conclusion is obtained as in Section IV, i.e it is more efficient to employ a higher order scheme.

Overall, no difference in the convergence behavior for time-dependent and time-independent operators in the inhomogeneous term, $\hat{\mathbf{G}}(t)$ is found. This can be rationalized as follows: the convergence is determined by the fastest timescale of the dynamics, i.e. by

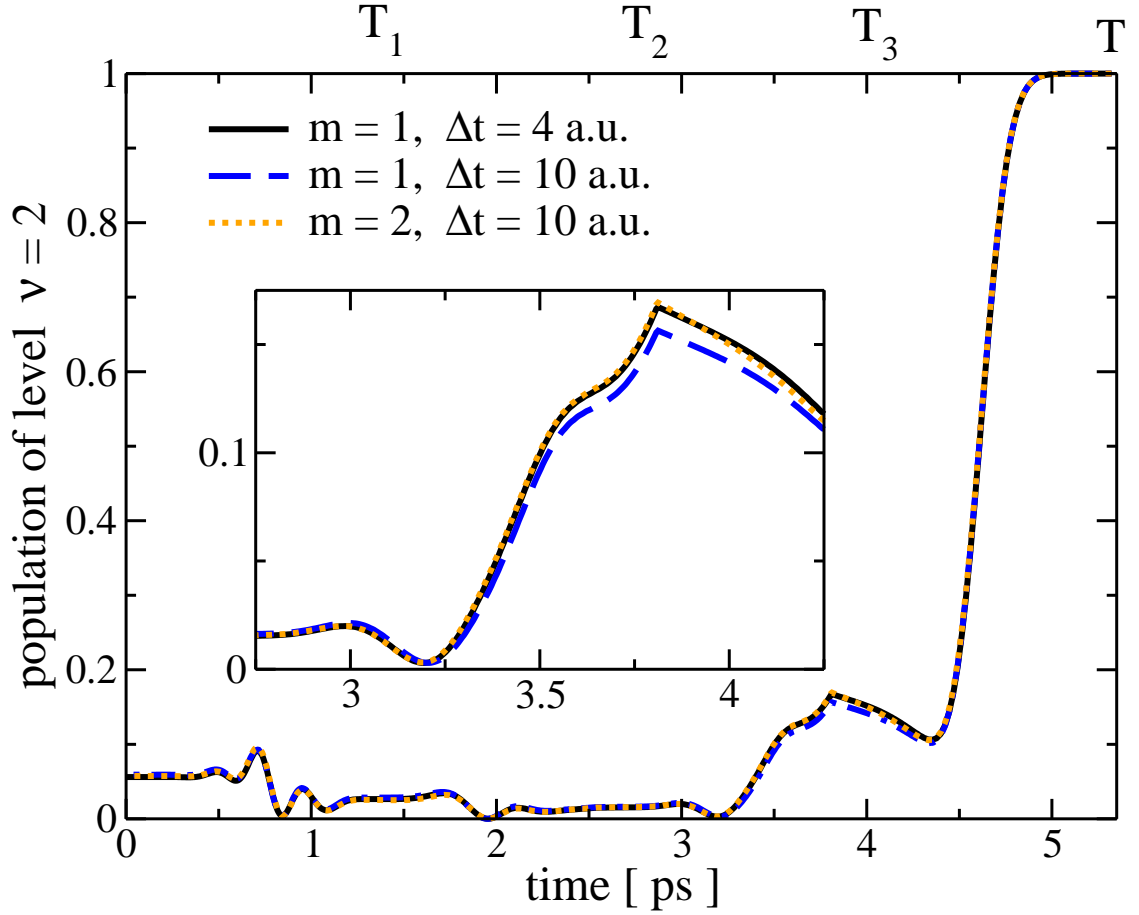


FIG. 9: (color online) (a) Time-dependent population of the final target level $\nu = 2$: Converged results in first and second orders for the largest possible time step (black solid and orange dotted lines). Also shown is a non-converged result in first order (blue dashed line) - the deviations from the converged solutions are evident in the insert.

order m	time step Δt	N_{Cheby}	applications of $\hat{\mathbf{H}}$	CPU time
1	4 a.u.	8	495.000	0.72 s
2	10 a.u.	10	264.000	0.62 s

TABLE IV: CPU time required to obtain converged solutions in first and second order for a total propagation time of 5.4 ps

the rapid oscillations of the field. The time-dependence of the projection operator introduces a time-dependence which is much slower and hence does not affect convergence.

VI. CONCLUSIONS

A formal solution to the time-dependent inhomogeneous Schrödinger equation was derived based on an expansion of the inhomogeneous term. Three levels of Chebychev approximations are involved. (i) The first one yields the Chebychev propagator where the argument of the Chebychev polynomials is the Hamiltonian. Truncating the expansion at the desired order m , the formal solution is subjected to a spectral representation with Chebychev polynomials. A propagation scheme similar to the standard Chebychev propagator for homogeneous Schrödinger equations is then obtained: Instead of $e^{-i\hat{H}\Delta t}$ a function $f_m(\hat{H})$ is expanded in Chebychev polynomials. While for the exponential, the expansion coefficients can be calculated analytically, they need to be obtained numerically for f_m . This is easily achieved by Fast Cosine Transformations, utilizing the definition of Chebychev polynomials as powers of cosines. (ii) The second level expands the inhomogeneous state vector $|\Phi(t)\rangle$ in Chebychev polynomials within each integration time interval $[0, \Delta t]$. The argument of this expansion is the rescaled time \bar{t} covering the interval. This Chebychev approximation can be easily applied only if $|\Phi(t)\rangle$ is known analytically. If $|\Phi(t)\rangle$ is determined numerically on sampling points covering the global propagation time interval $[0, T]$ as in the present application the Chebychev expansion is replaced by a Taylor expansion based on numerical derivatives at the beginning of each time step. (iii) The numerical calculation of the derivatives requires a third level of Chebychev approximation where the argument is the time t covering the global propagation time interval $[0, T]$. This implies a non-equidistant time grid where the derivatives are evaluated according to the procedure described in Ref. [16]. This expansion overcomes the numerical error introduced by non-zero boundary values of the inhomogeneous state vector $|\Phi(t)\rangle$ at $t = 0$ and $t = T$. An alternative based on equidistant time steps employs Fast Fourier Transforms and multiplication in frequency domain. However, in that case the errors introduced at the boundary of the time grid build up. Therefore this scheme is limited to low order where only first or second derivatives are required.

An even more approximate solution to the time-dependent inhomogeneous Schrödinger equation is obtained by rewriting the formal solution explicitly in terms of a Taylor expansion. The propagator then consists of the standard exponential term plus time derivatives of the inhomogeneous terms. This approximation is numerically less efficient than the propagator for the full formal solution. Moreover, it may become unstable in optimal control

applications where the inhomogeneous term often is highly oscillatory and the numerical evaluation of derivatives by FFT becomes difficult. The main advantage of this propagation scheme lies in the fact that it requires very little modification of existing standard Chebychev propagation codes.

Both Chebychev propagation schemes were tested in two optimal control applications. OCT with a state-dependent constraint [7], e.g. maximizing population in an allowed subspace of the Hilbert space, yields a time-independent operator in the inhomogeneous term while an explicitly time-dependent operator is obtained in OCT with a time-dependent target [3, 4, 5, 6]. Convergence of the propagation schemes was demonstrated for both applications. The convergence behavior was studied in detail as a function of the order of the solution and the required number of time steps for a given overall propagation time. For applications with a fast time-dependence such as OCT, a low order scheme with a small time step and evaluation of the time derivatives by FFT was found to be the best choice. For applications with a slow time-dependence or time-independent Hamiltonians such as reactive scattering calculations where large time steps are permissible, a high-order scheme is numerically most efficient. This reflects that the propagation scheme based on a global representation of the inhomogeneous term. It is this regime where the new propagator can best unfold its power.

The new Chebychev propagator provides a stable and accurate numerical solution to the time-dependent inhomogeneous Schrödinger equation. It is most efficient for high order and large time steps. Ideally an inherent time-dependence of the Hamiltonian should also be incorporated into the Chebychev scheme. This is the subject of a further study.

Acknowledgments

We would like to thank José Palao for stimulating discussions. Financial support from the Deutsche Forschungsgemeinschaft within the Emmy-Noether grant KO 2302/1-1 (CPK) and within SFB 450 (MN,RK) is gratefully acknowledged. The Fritz Haber Center is supported by the Minerva Gesellschaft für die Forschung GmbH München, Germany.

APPENDIX A: PROOF OF THE EQUIVALENCE OF EQS. (6) AND (17)

It is shown by induction that the formal solution, Eq. (6), and Eq. (17) are equivalent. Writing Eqs. (6) and (17) for $m = 1$, one obviously obtains in both cases the equation of the first order, Eq. (10). We assume that Eqs. (6) and (17) are equivalent in order $m - 1$, i.e.,

$$|\psi(t)\rangle_{(m-1)} = \sum_{j=0}^{m-2} \frac{t^j}{j!} |\lambda^{(j)}\rangle + \hat{\mathbf{F}}_{m-1} |\lambda^{(m-1)}\rangle = e^{-i\hat{\mathbf{H}}t} |\psi_0\rangle + \sum_{j=0}^{m-2} \hat{\mathbf{F}}_{j+1} |\Phi^{(j)}\rangle, \quad (\text{A1})$$

let us now prove that they are equivalent in order m .

$$\begin{aligned} |\psi(t)\rangle_{(m)} &= \sum_{j=0}^{m-1} \frac{t^j}{j!} |\lambda^{(j)}\rangle + \hat{\mathbf{F}}_m |\lambda^{(m)}\rangle \\ &= \sum_{j=0}^{m-2} \frac{t^j}{j!} |\lambda^{(j)}\rangle + \frac{t^{m-1}}{(m-1)!} |\lambda^{(m-1)}\rangle + \hat{\mathbf{F}}_m \left((-i\hat{\mathbf{H}}) |\lambda^{(m-1)}\rangle + |\Phi^{(m-1)}\rangle \right) \\ &= \sum_{j=0}^{m-2} \frac{t^j}{j!} |\lambda^{(j)}\rangle + \hat{\mathbf{F}}_m |\Phi^{(m-1)}\rangle + \left(\hat{\mathbf{F}}_m (-i\hat{\mathbf{H}}) + \mathbb{1} \frac{t^{m-1}}{(m-1)!} \right) |\lambda^{(m-1)}\rangle \end{aligned} \quad (\text{A2})$$

We continue by showing that $\hat{\mathbf{F}}_{m-1} = \hat{\mathbf{F}}_m (-i\hat{\mathbf{H}}) + \mathbb{1} \frac{t^{m-1}}{(m-1)!}$,

$$\begin{aligned} \hat{\mathbf{F}}_m (-i\hat{\mathbf{H}}) + \mathbb{1} \frac{t^{m-1}}{(m-1)!} &= (-i\hat{\mathbf{H}})^{-(m-1)} \left(e^{-i\hat{\mathbf{H}}t} - \sum_{j=0}^{m-2} \frac{(-i\hat{\mathbf{H}}t)^j}{j!} - \frac{(-i\hat{\mathbf{H}}t)^{m-1}}{(m-1)!} \right) + \mathbb{1} \frac{t^{m-1}}{(m-1)!} \\ &= (-i\hat{\mathbf{H}})^{-(m-1)} \left(e^{-i\hat{\mathbf{H}}t} - \sum_{j=0}^{m-2} \frac{(-i\hat{\mathbf{H}}t)^j}{j!} \right) - (-i\hat{\mathbf{H}})^{-(m-1)} \frac{(-i\hat{\mathbf{H}}t)^{m-1}}{(m-1)!} + \mathbb{1} \frac{t^{m-1}}{(m-1)!} \\ &= (-i\hat{\mathbf{H}})^{-(m-1)} \left(e^{-i\hat{\mathbf{H}}t} - \sum_{j=0}^{m-2} \frac{(-i\hat{\mathbf{H}}t)^j}{j!} \right) - \mathbb{1} \left(\frac{t^{m-1}}{(m-1)!} - \frac{t^{m-1}}{(m-1)!} \right) \\ &= (-i\hat{\mathbf{H}})^{-(m-1)} \left(e^{-i\hat{\mathbf{H}}t} - \sum_{j=0}^{m-2} \frac{(-i\hat{\mathbf{H}}t)^j}{j!} \right) = \hat{\mathbf{F}}_{m-1}. \end{aligned}$$

Equation (A2) thus becomes

$$|\psi(t)\rangle_{(m)} = \sum_{j=0}^{m-2} \frac{t^j}{j!} |\lambda^{(j)}\rangle + \hat{\mathbf{F}}_{m-1} |\lambda^{(m-1)}\rangle + \hat{\mathbf{F}}_m |\Phi^{(m-1)}\rangle.$$

Making use of our assumption, Eq. (A1), we obtain

$$\begin{aligned} |\psi(t)\rangle_{(m)} &= e^{-i\hat{\mathbf{H}}t} |\psi_0\rangle + \sum_{j=0}^{m-2} \hat{\mathbf{F}}_{j+1} |\Phi^{(j)}\rangle + \hat{\mathbf{F}}_m |\Phi^{(m-1)}\rangle \\ &= e^{-i\hat{\mathbf{H}}t} |\psi_0\rangle + \sum_{j=0}^{m-1} \hat{\mathbf{F}}_{j+1} |\Phi^{(j)}\rangle. \end{aligned}$$

This concludes the proof.

- [1] D. Neuhauser, M. Baer, R. S. Judson, and D. J. Kouri, *Comput. Phys. Comm.* **63**, 460 (1991).
- [2] D. Neuhauser, *Chem. Phys. Lett.* **200**, 173 (1992).
- [3] A. Kaiser and V. May, *J. Chem. Phys.* **121**, 2528 (2004).
- [4] I. Șerban, J. Werschnik, and E. K. U. Gross, *Phys. Rev. A* **71**, 053810 (2005).
- [5] A. Kaiser and V. May, *Chem. Phys.* **320**, 95 (2006).
- [6] J. Werschnik and E. K. U. Gross, *J. Phys. B* **40**, R175 (2007).
- [7] J. P. Palao, R. Kosloff, and C. P. Koch, *Phys. Rev. A* **77**, 063412 (2008).
- [8] D. Neuhauser and M. Baer, *J. Chem. Phys.* **91**, 4651 (1989).
- [9] W. Zhu, J. Botina, and H. Rabitz, *J. Chem. Phys.* **108**, 1953 (1998).
- [10] J. P. Palao and R. Kosloff, *Phys. Rev. A* **68**, 062308 (2003).
- [11] Y. Ohtsuki, G. Turinici, and H. Rabitz, *J. Chem. Phys.* **120**, 5509 (2004).
- [12] R. Kosloff, *J. Phys. Chem.* **92**, 2087 (1988).
- [13] R. Kosloff, *Annu. Rev. Phys. Chem.* **45**, 145 (1994).
- [14] H. Tal-Ezer and R. Kosloff, *J. Chem. Phys.* **81**, 3967 (1984).
- [15] R. Baer, *Phys. Rev. A* **62**, 063810 (2000).
- [16] D. Dunn, *Comput. Phys. Comm.* **96**, 10 (1996).
- [17] S. J. Park, S. W. Suh, Y. S. Lee, and G. H. Jeung, *J. Molec. Spec.* **207**, 129 (2001).